

# Influence of thermal treatments on Ag Sn Cu powders in order to reduce mercury contents in dental amalgam

CORA BRACHO-TROCONIS\*<sup>†</sup>, PIERRE COLON<sup>‡</sup>, JEAN-DOMINIQUE BARTOUT<sup>†</sup>, YVES BIENVENU<sup>†</sup>

\* *Laboratoires Septodont, France*

<sup>†</sup> *Centre Des Materiaux P.M. Fourt, Ecole Nationale Supérieure Des Mines De Paris, France*

<sup>‡</sup> *Hotel Dieu, Université Denis Diderot, Service d'Odontologie Garancière, France*

The mercury content of dental amalgams is a controversial subject with regard to the biological properties of these materials. The object of this study is to optimize the thermal treatments performed on an experimental powder in order to obtain a low mercury ratio (41% by weight) while preserving the desirable clinical qualities of the material. Using atomized powder, two types of thermal treatments are performed: A1, to obtain a partially annealed structure and A2, to obtain a complete homogenization. The kinetics of the amalgamation reaction is mainly evaluated by X-ray diffraction to identify the newly formed phases as a function of setting time. Mechanical properties are evaluated according to the ISO norms at 37 °C.

Metallographical examination of the amalgams shows a Ag-Hg phase which acts as a matrix incorporating the Cu-Sn and Ag-Sn compounds. The setting kinetics of the A1 amalgams is linear and slightly more rapid than that of the A2 amalgam. The mechanical properties of the amalgams are significantly improved regarding the higher mercury content commercial amalgams.

A specific thermal treatment permits us to slow down the diffusion of mercury between the different intermetallic compounds into the powder. The final amalgam composition, thus, most approaches the stoichiometric ratio calculated from a quaternary diagram.

© 2000 Kluwer Academic Publishers

## 1. Introduction

Dental amalgams constitute almost 75% of all restorative materials used in dental practice [1]: they are the result of the combination of mercury and a silver copper tin powder. Intermetallic compounds obtained during this reaction (Ag-Hg, Cu-Sn) determine the mechanical properties of these materials.

However, mercury release is a subject of controversy [2–4]. The biologic properties of this class of materials could obviously be improved by reducing the mercury content. One way to achieve that is to optimize the powder characteristics, morphology and particle size distribution. The use of spherical powders can be considered as the first step to reduce the mercury content: a weight percentage of 43% of mercury can be obtained instead of 50% for the lathe cut particles used previously.

The aim of this study is to reduce more these values in respect of handling in clinical practice. Most particularly, the setting time has to be long enough to allow the clinical procedure of insertion and carving of the amalgam in the tooth cavity.

The influence of thermal treatments of powders on the kinetics of setting reaction is investigated in order to

conciliate a low mercury rate and improved handling properties.

## 2. Starting materials and experimental methods

The silver based gas atomized powders with an average particle size ( $d_{50}$ ) of the order of 30  $\mu\text{m}$  were produced by Nanoval (Berlin-FRG) under a proprietary process [5]. The powders are roughly spherical and exhibit a wide dispersion in size (Fig. 1).

The nominal composition was :

Ag: 59.5 wt%      Sn: 27.5 wt%      Cu: 13 wt%

The atomization and heat treatment were carried out under inert atmosphere in order to control the surface oxidation of metal particles. Two types of powder heat treatment were compared: a soft anneal to relieve the internal stresses occurring in the powders as the result of the rapid cooling of the fine droplets during gas atomization and a high temperature anneal which caused the phases to also undergo microstructural coarsening and a full return to equilibrium.

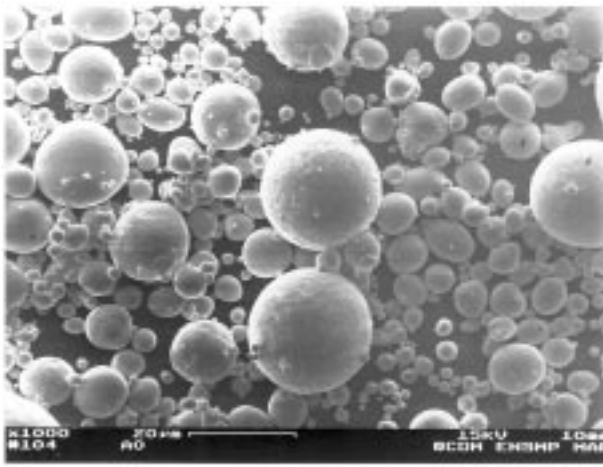


Figure 1. Ag-Sn-Cu gas atomized powders.

The solidus (470 °C) and the liquidus (520 °C) temperatures of the alloy were measured by differential thermal analysis (DTA) with a Setaram TG/DTA 92 thermal analyser using inert alumina crucibles with a heating rate of 10 °C/min under flowing argon to minimize volatilization losses of silver or oxidation of tin. The thermogram of the as atomized powders also evidenced a solid state reaction, a return to equilibrium evidenced by an exothermal peak in a temperature range of 125 °C to 180 °C (presumably a transformation of the “Ag<sub>4</sub>Sn” type of phase into “Ag<sub>3</sub>Sn”). The solidus and liquidus temperatures are in rough agreement with available phase diagram information [6]. The three experimental powders are subsequently designated as:

- A0: such as atomized
- A1: soft annealed
- A2: fully annealed

Amalgams were produced according to ISO standard [7] and stored at 37 °C until used.

The metallographic examinations were carried out on polished sections of the powders (as atomized or annealed), embedded in Epofix<sup>®</sup> resin and on the polished sections of amalgams. Polishing was effected using a grade 1200 silicon carbide, then 7 and 3 μm diamond paste polishing discs and a final polishing with a suspension of colloidal silica. Optical metallographs were taken with a Zeiss Axiovert light microscope. Scanning electron microscopy was performed using a high resolution Zeiss DSM 982 Gemini scanning electron microscope equipped with a Noran Instruments solid state microanalytical X-ray detector. EPMA (electron probe microanalysis) was performed on an automated Cameca SX50 microanalyser equipped with SAM’X data processing (WDS mode).

Two methods were achieved to record the progress of the amalgamation reaction from 3 min to several hours after introducing mercury and the silver bearing powders in contact:

1. X-ray diffraction using cobalt K $\alpha$  radiation and an automated  $\theta/2\theta$  goniometer, D500 from Siemens,

equipped with a linear multichannel detector from ELPHYSE. Acquisition was performed on an angular range of 14° in 2 $\theta$  which allowed to encompass both characteristic diffraction lines from the parent phases and from the Ag-Hg phase at 2 min intervals.

X-ray diffraction was also used to study the evolution of the constitution of the silver bearing powders during the heat treatments.

2. Microhardness measurements with a Vickers indenter under a load of 300 g. Each point on the results was the average of 5 measurements.

The compressive room temperature rupture strength of the amalgams was determined at regular intervals starting 5 min after condensation of the dental amalgams using a Zwick 10t universal tester (screw driven) equipped with a 1 t load cell and with a linear LVDT inductive displacement sensor.

The creep of the amalgams was studied one week after condensation according to the ISO standard [7] at 37 °C.

### 3. Results

#### 3.1. Powders examination

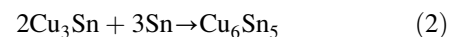
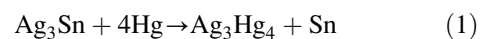
Metallographic structure of the three experimental powders are shown on Fig. 2. Figs 2a and 2b suggest no modification of the structure between powders A0 and A1. However, X-ray diffraction demonstrates the transformation of Ag<sub>4</sub>Sn phase into Ag<sub>3</sub>Sn phase. Fig. 2c exhibits the transformation of the micro structure (coarsening of the dark phase identified in the A2 heat treatment conditions).

Our findings relative to the stability of Ag-Sn compounds are in agreement with the ternary Ag-Cu-Sn phase diagrams. Liquidus for the atomized powders and 37 °C isothermal section for the heat treated powder A1 and A2 are shown in Fig. 3.

#### 3.2. Metallographic structure of amalgams

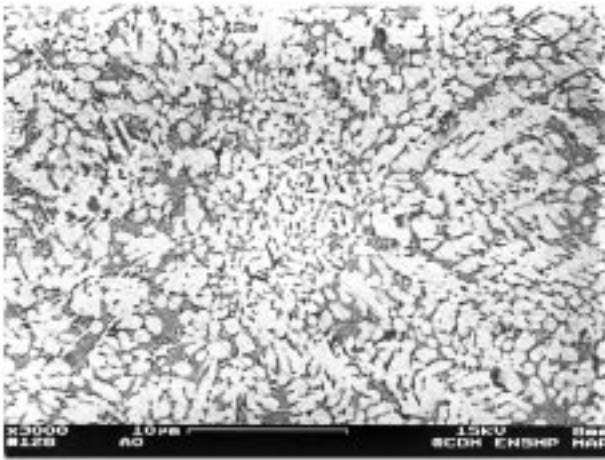
The amalgams are prepared with a ratio of 41 wt% of mercury and 59 wt% of powders. Usually a content of 43 wt% is considered as minimal. The structure of the amalgams shows a continuous Ag-Hg matrix in which the spherical powders are embedded, the smaller particles being often disintegrated by their reaction with mercury (Fig. 4).

Observation of polished sections at higher magnification shows that the outer surface of the Ag-Sn-Cu particles is modified, and microanalysis suggests the following setting reactions :

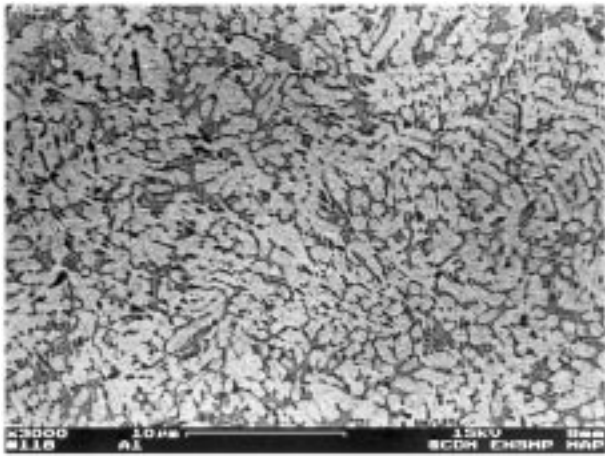


This justifies the empirical finding that the addition of Cu to the basic Ag-Sn alloys suppresses the  $\gamma_2$  (Hg-Sn) phase formation during amalgamation [8].

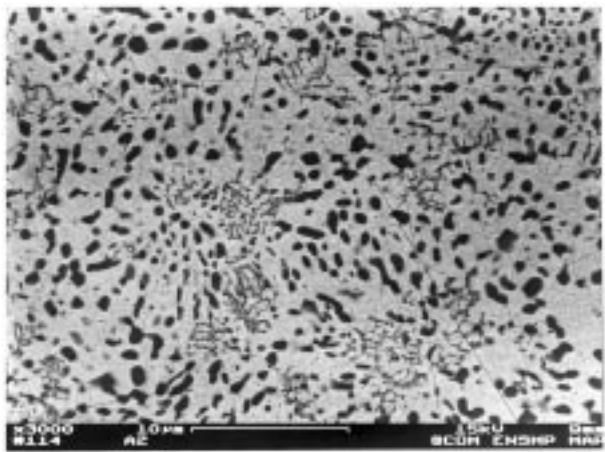
The Cu<sub>6</sub>Sn<sub>5</sub> compounds are mainly located in the reacted circumference of the particles when seen in the SEM using backscattered electron contrast, the interface between the dark (Cu-Sn) and the grey (Ag-Sn) phases in



(a)



(b)



(c)

Figure 2. SEM micrographs, backscattering electrons of polished cross section of powders, (a) as atomised, (b) soft annealed A1, (c) fully annealed A2.

that zone appears as a preferential path for the attack by the mercury rich white continuous phase (matrix), Fig. 5.

The average matrix composition was 50 at%Hg, 45 at%Ag and about 2 at% for both Sn and Cu which fits well with the reported  $Ag_3Hg_4$  binary stoichiometry. The matrix grain size is about 2  $\mu m$ .

The issue of mercury is illustrated by Figs 4 and 5: the

ratio powder to mercury (powder contents/powder contents: mercury contents/powder contents) determines the volume of the matrix in relation with the specific surface of the powder.

Other  $Cu_6Sn_5$  are found amid Ag-Hg phase. The size and distribution of this phase varies with amalgam's powder heat treatment and composition as found by other authors [9, 10].

This matrix volume fraction has to be minimized in order to improve mechanical properties and to reduce the presence of mercury in the alloy: the Ag-Hg intermetallic characteristics are reputed inferior to those of the Cu-Sn and Ag-Sn intermetallics. The mechanical properties of dental amalgams are controlled by the Ag-Hg matrix. However, the cohesion of amalgam requires a good embedment of the particles and a surface reaction between powder and mercury.

### 3.3. Setting reaction and consolidation of amalgam

- Results of the X-ray study of the formation of the  $Ag_3Hg_4$  product phase are shown on Fig. 6 for A1 and A2. The powder A0 combined with 41 wt% of mercury does not produce an homogeneous mixture suitable for handling on the diffractometer template.

We can see that from 10 min after the end of trituration to one hour, the setting reactions kinetic is about linear. A possible explanation is that the limiting reaction is the dissolution of the phase Ag-Sn in liquid mercury and not solid state diffusion (usually associated with a parabolic kinetic law).

This could correspond to the transfer of the elements (Ag primarily) of a solid into a liquid as long as mercury is in sufficient proportion. This dissolution is rapid and therefore does not depend on time. After a long range of time, when there is no more sufficient mercury, the reaction kinetic slows down. Indeed, it is what we have observed.

It is difficult to compare the kinetics of amalgamation of A1 and A2 even if powder A1 shows a slightly faster reaction.

- Results of microhardness measurements (Fig. 7) confirm that amalgam A1 exhibits a faster reaction kinetics than the A2 ones. It is important to specify that the reaction is not complete after one hour. Actually, the microhardness after one week increases to 200 Hv for both amalgams.
- Results of compressive strength (Fig. 8) are in agreement with previous results. However, after one hour, amalgam A2 becomes more resistant than A1. Nevertheless, these values are significantly superior to values obtained with commercially available amalgams with a mercury content of 43% [11].

The plot exhibiting the compressive fracture strength according to time shows us that, from 24 h, the evolution of this mechanical property is slower and slower. This property being linked to the microstructure, we can think that the reaction develops slower and slower. Thereby, it

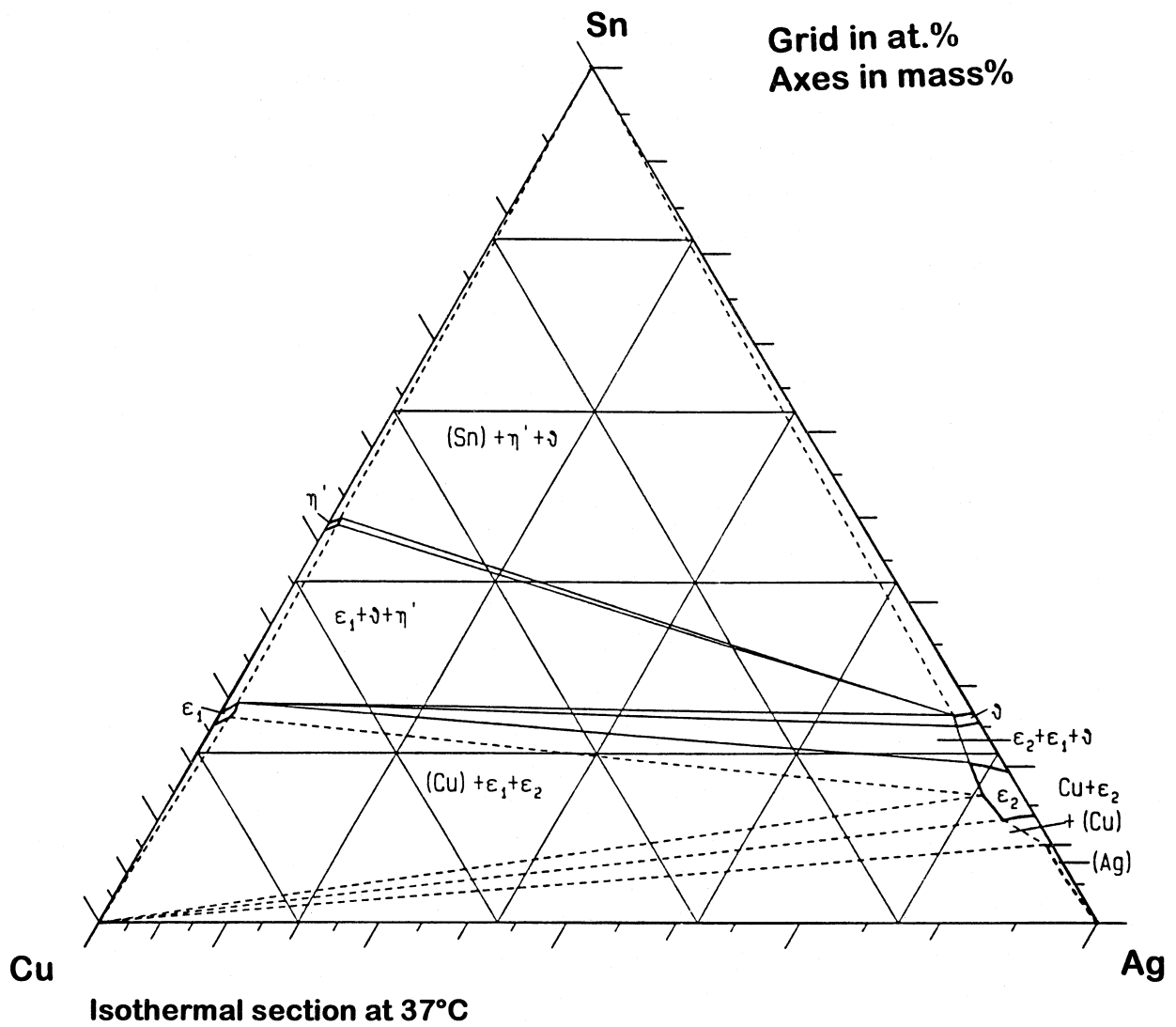
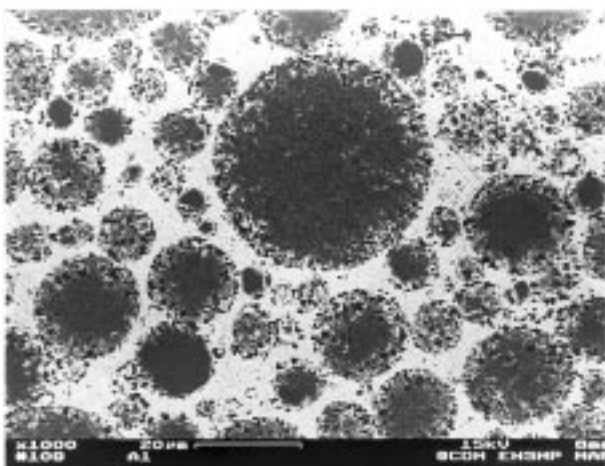
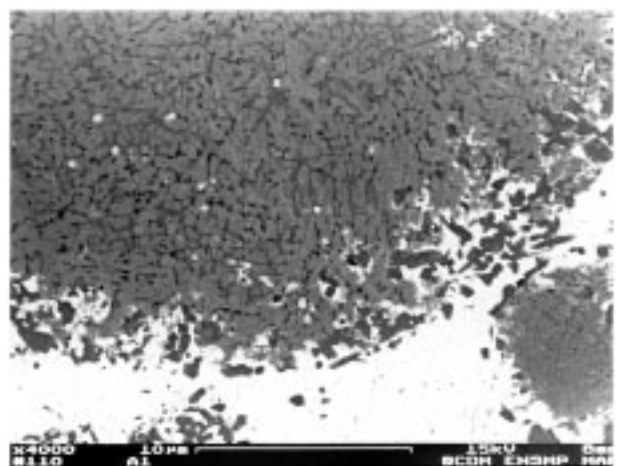


Figure 3 Ag-Sn-Cu ternary diagram, isothermal section at 37°C.

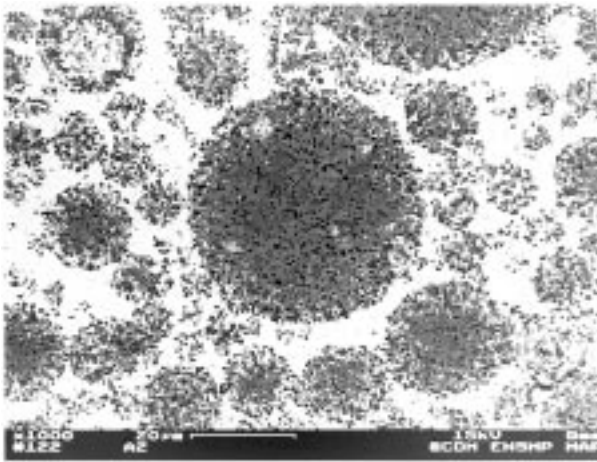


(a)

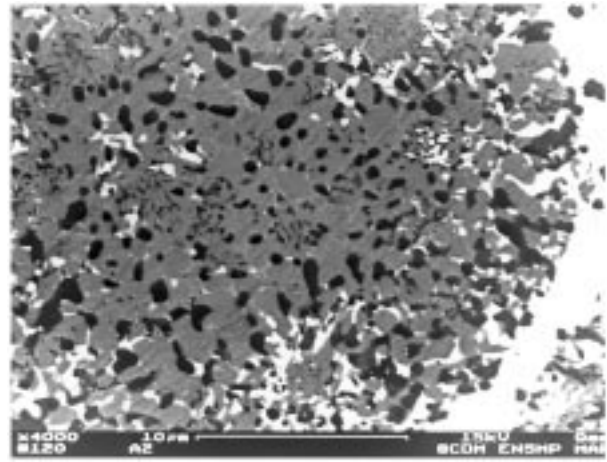


(b)

Figure 4. SEM micrographs, backscattering electrons, of polished Al amalgam cross section, after setting; (a) *low magnification* : the residual spherical particles of powder are embedded in a continuous Ag-Hg matrix; (b) *high magnification* : the interface between the spherical particle and the Ag-Hg matrix.



(a)



(a)

Figure 5 SEM micrograph, backscattering electrons, of polished A2 amalgam cross section, after setting: (a) low magnification: the structure of the amalgam is similar to those obtained on Fig. 4a; (b) high magnification: the  $\text{Cu}_6\text{Sn}_5$  compounds do not form a network and although mercury diffusion is slower.

results in a quasi steady state (or damped conditions) of solid diffusion.

### 3.4. Creep testing of stabilized amalgams.

The ISO test (Fig. 9) is carried out 7 days after trituration on five samples aged, at 37 °C.

It has been suggested that the lower creep in this type of amalgams (called High Copper Single Composition Amalgams, HCSC) is due to an increase in  $\text{Cu}_6\text{Sn}_5$  in the material after setting [10].

## 4. Discussion

The results and the mechanisms proposed in section 3.2. for the amalgamation allow to establish the range for the mercury content. Mercury acts as a binder like the liquid

phase in a liquid phase sintering process. Although the reactive nature of the process dominates the densification process, we also attempt to draw a parallel with more classical liquid phase sintering processes (in spite of the difference in temperature: ambient temperature for amalgamation and above 1000 °C for the classical sintering reactions).

### 4.1. Theoretical considerations on powder composition and on mercury ratio

The maximum amount for mercury within an amalgam is the one that corresponds to its full reaction with the silver based powder. An excess of mercury may lead to the presence of free mercury or to the formation of the Hg-Sn ( $\gamma_2$ ) intermetallic compound. Using reaction (1) and (2),

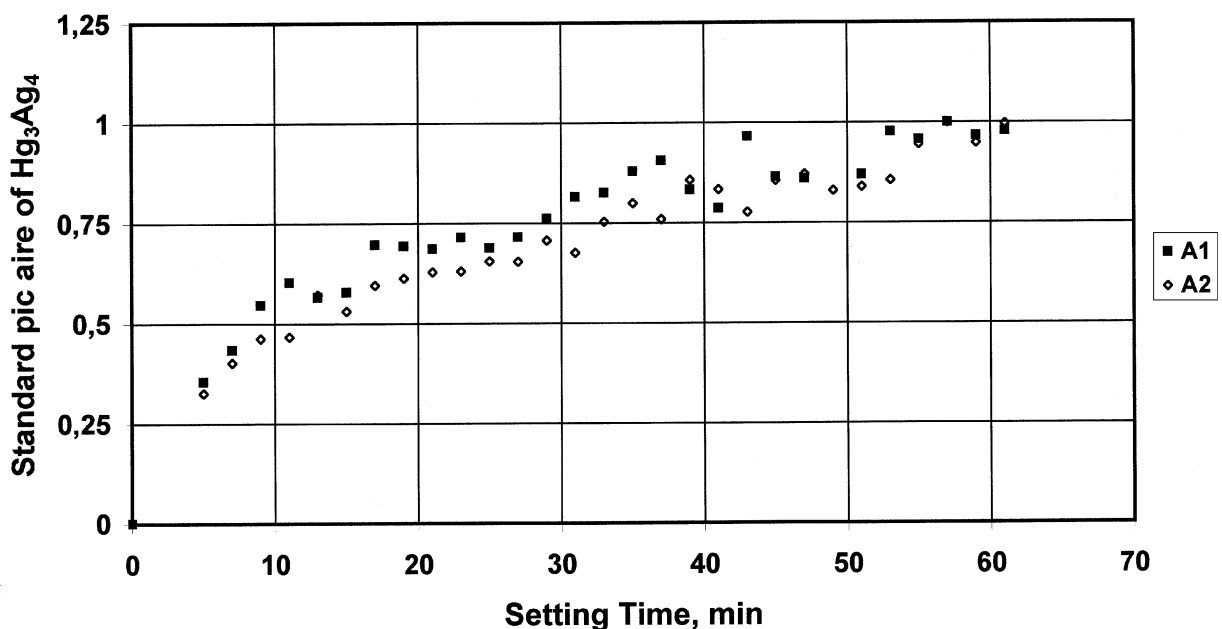


Figure 6 Results of the X-ray study : formation of  $\text{Ag}_3\text{Hg}_4$  as a function of setting time.

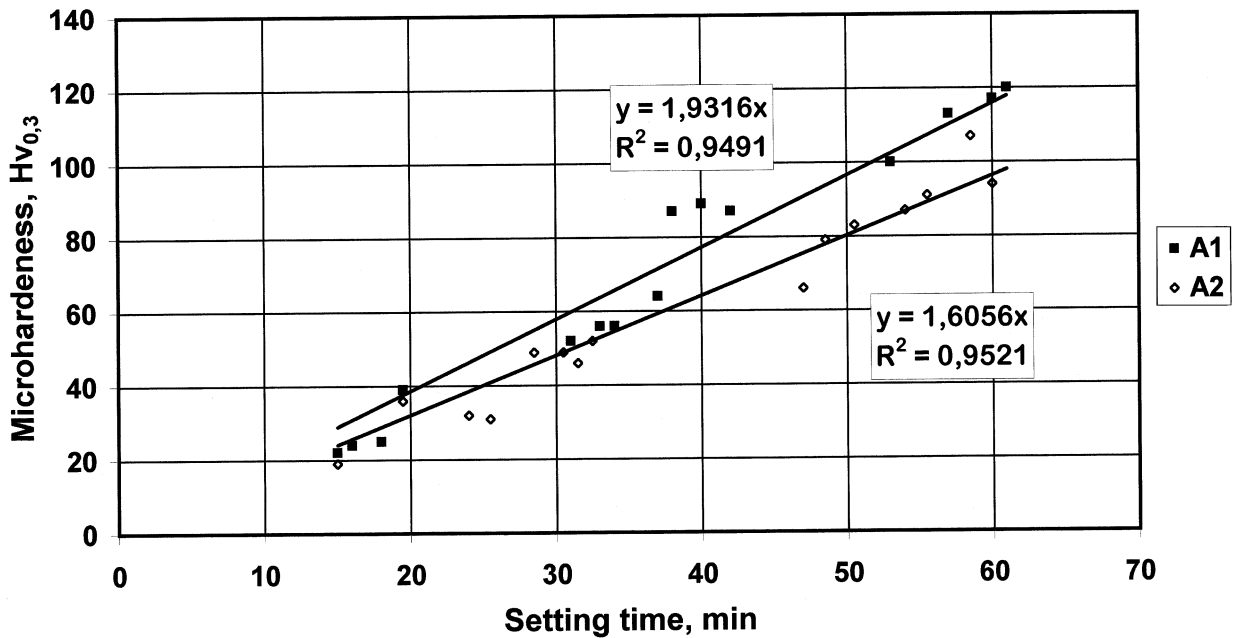


Figure 7 Evolution of microhardness of amalgams as a function of setting time.

the maximum content may be obtained and we also propose a graphical solution in Fig. 10.

The A1 and A2 powder constitution is a juxtaposition of the  $Cu_3Sn$  and  $Ag_3Sn$  intermetallic compounds. After amalgamation, the silver-tin intermetallic is no longer to be found. All the tin is then combined as  $Cu_6Sn_5$  and all the silver as «Hg-Ag», the binder phase in the reacted amalgam. The graphical construction in Fig. 11 leads to a theoretical molar composition of the powder:  $Ag_{0,45}-Sn_{0,25}-Cu_{0,3}$ , which translates into 50 wt%Ag, 30.5 wt%Sn and 19.6 wt%Cu which differs significantly (for the silver content) from the actual composition.

A much closer argument is reached when we make the assumption that the Ag-Sn intermetallic composition is

that of  $Ag_4Sn$  (although the structure is that of  $Ag_3Sn$ . The stoichiometry range of  $Ag_4Sn$  allows it). We then arrive at a composition expressed in wt%: 56.1Ag, 26.5Sn, 16.73Cu. The maximum mercury content is then dictated by the reaction of all Ag to form  $Ag_3Hg_4$ : we arrive at 59.5 wt% for the actual composition (and 55% for the theoretical powder composition), which is far in excess of the actual mercury ratio in the amalgams. Indeed a large fraction of the powder mass is left seemingly unreacted (Figs 4 and 5).

The minimum binder (initially mercury from  $Hg_4Ag_5$ ) content is dictated by stereological considerations (the filling by mercury of the initial porosity in the “condensed” powder). For instance, with an initial relative (tapped) density of 0.6 for the silver based

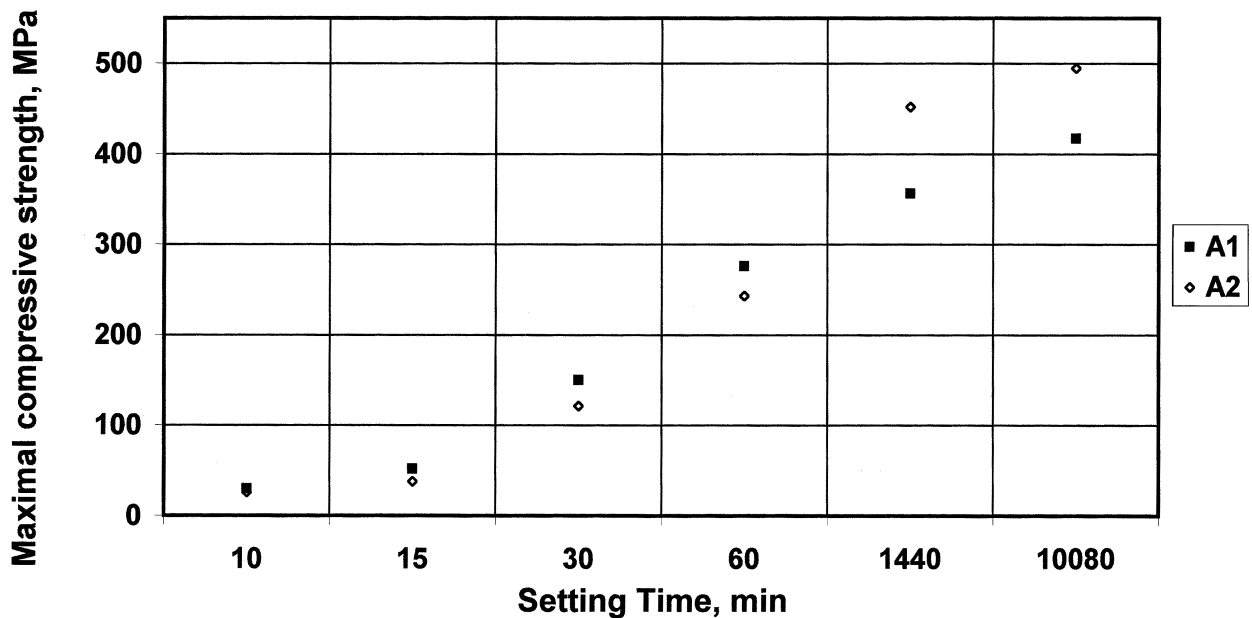


Figure 8 Evolution of compressive strength of the amalgams as a function of setting time.

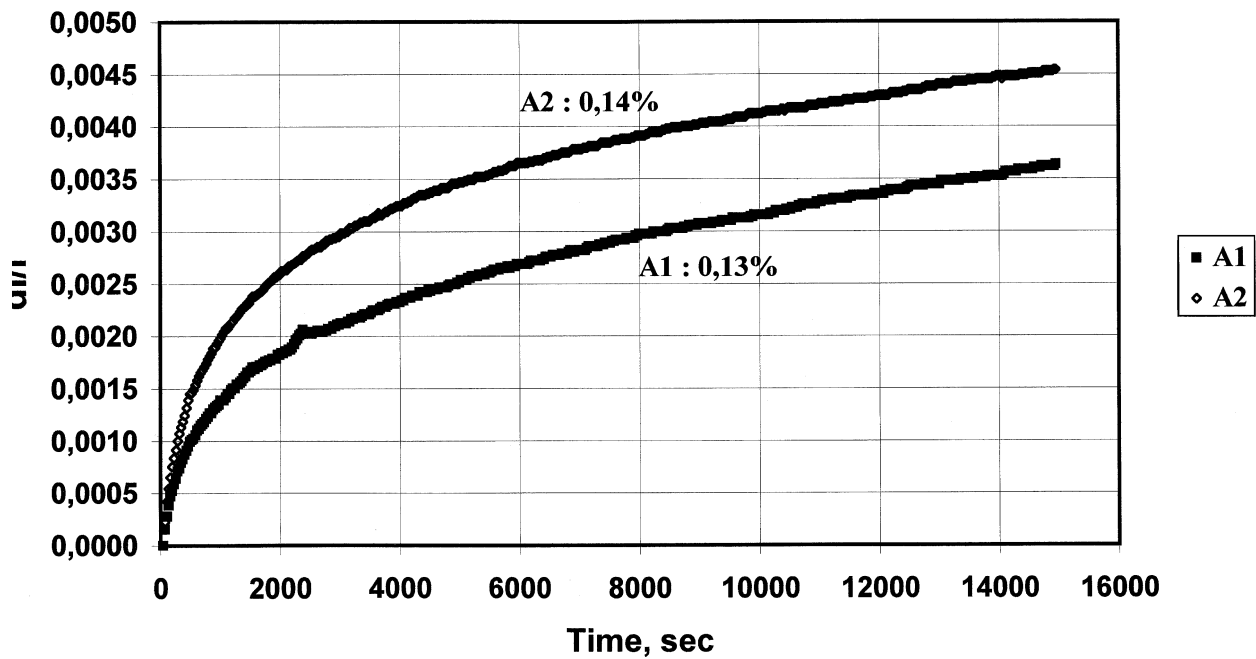


Figure 9 Evaluation of creep of stabilized amalgams according to ISO standard 1559.

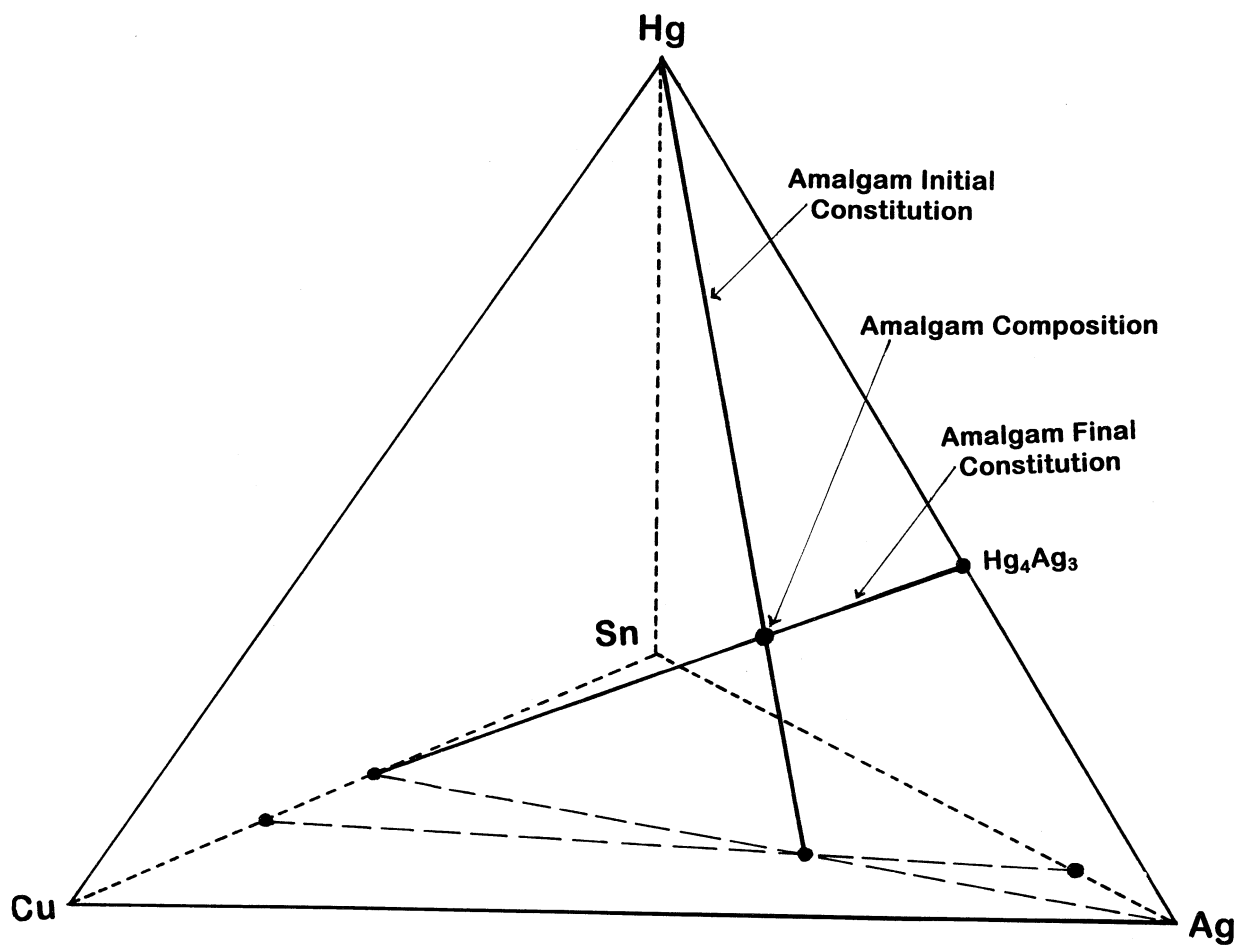


Figure 10 Schematic positioning of the powder alloy composition, of the amalgam's composition and of the binary intermetallic phases in the quaternary representation Ag-Cu-Sn-Hg.

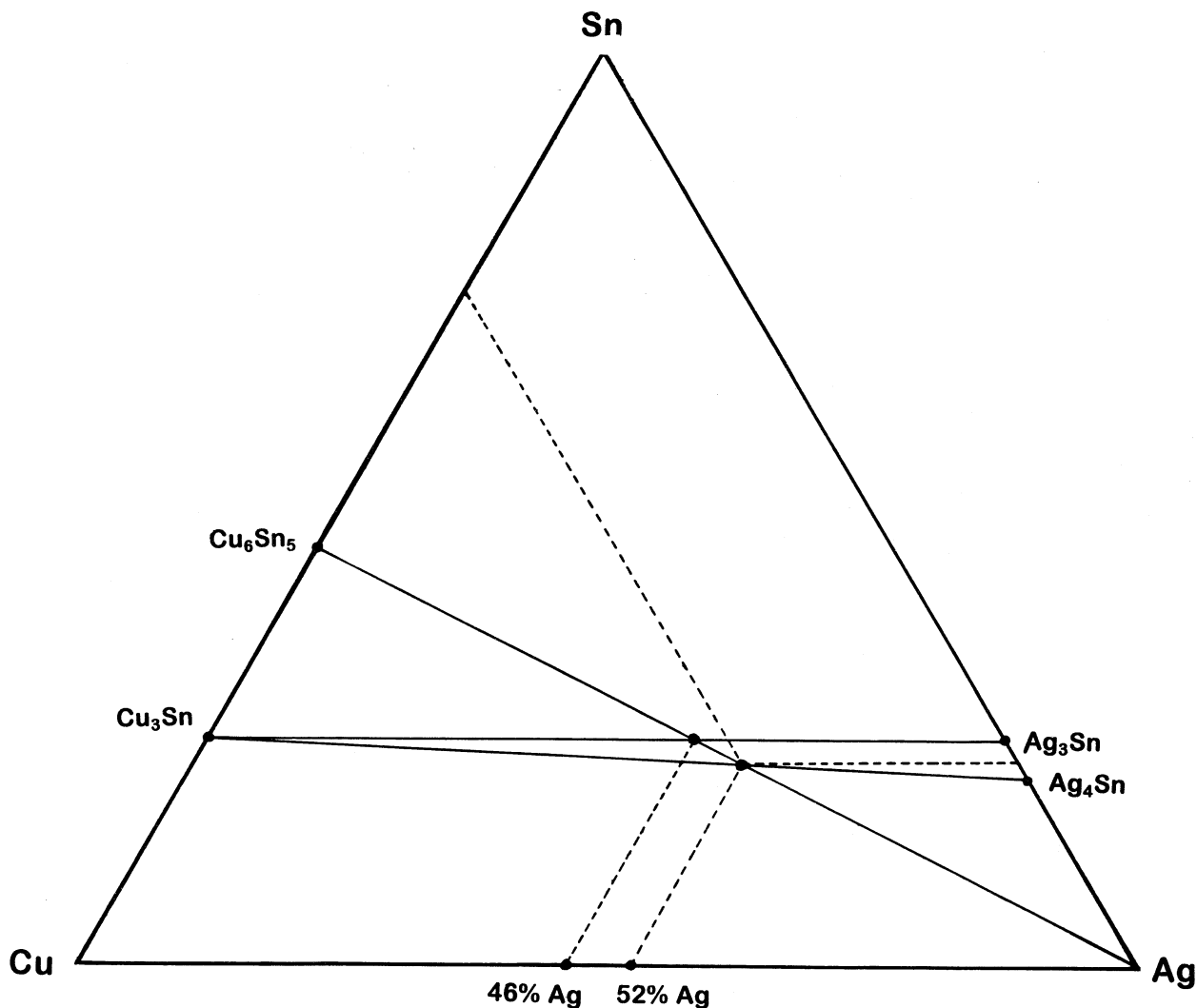


Figure 11 "Ideal" amalgam composition in the ternary representation Ag-Cu-Sn. Initial constitution:  $\text{Cu}_3\text{Sn}-\text{Ag}_4\text{Sn}$ . Final constitution:  $\text{Cu}_6\text{Sn}_5-\text{Ag}$  reacting with Hg.

powder, the minimum mercury content would be 47%, it decreases to 43% for a relative density of 0.65 for the powder and to reach the 38% mercury ratio, the relative density of the powder would then be of 0.7. The tapped density of the powder of this study is in excess of 65% and this may well justify the fact that we were able to decrease the mercury content down to 38%, in agreement with theoretical consideration.

The powder being both spherical and essentially intermetallic, is incompressible (at room temperature). The void fraction is then solely dictated by the size distribution. It is known that a wide size distribution increases packing density, small particles fitting within the interaction left between the larger ones.

German [12] indicates the optimum mixing of graded particle sizes and suggest ways to increase the packing fraction to 0.86. Further action on size distribution is to be investigated to further decrease the mercury content.

The densification process identified there is related to liquid phase sintering, the liquid phase being of transient nature. Such processes are well known in the field of brazing and repair-brazing and especially in the reconditioning of nickel base superalloys [13–16] The differences between amalgamation and these applica-

tions pertain to the temperature and to the fact that with nickel base superalloys, the liquid phase forms upon heating and disappears by solid state diffusion of the melting point depressor (boron or silicon) with the formation of a small amount of intermetallics (borides, silicides). In the amalgam we propose, the liquid phase disappears by a capillarity driven penetration of mercury within the particles along the  $\text{Ag}_3\text{Sn}/\text{Cu}_3\text{Sn}$  interfaces, reacts with the silver intermetallic according to reaction (1), the silver diffusing back into mercury where it reacts to form  $\text{Ag}_3\text{Hg}_4$  (solid phase). The kinetics of amalgamation followed by the various methods presented in section 2 or 3.3 slows down when the liquid matrix turns a viscous solid/liquid mixture.

Although most of the amalgamation reaction is completed in less than one hour, the last drops of mercury would react hours or days after condensation.

The influence of heat treatment (amalgamation reaction slower with A2) on powders before mercury addition may be justified in terms of the coarsening of the microstructure after the A2 heat treatment: the specific interfacial area of the intermetallic in A2 is lower which slows down the penetration of mercury.



## 5. Conclusion

Using an improved particle size distribution and finer particle sizes, it has been possible to reduce the mercury content in dental amalgams. In addition to the effect of mercury ratio (the 41% value tested with success in the present study being probably a record low value), we investigated the effect of different powder heat treatments and showed they had an effect on the kinetics of amalgamation and also on the final amalgam hardness.

The amalgamation reactions were analysed and mechanisms are proposed for the reaction of mercury with the copper and silver brass in the initial powders. Stoichiometry considerations and stereological calculations lead to predict maximum and minimum values of the mercury content.

Indeed our 41% minimum mercury content in the amalgam is quite close to the minimum. Further reductions in mercury may be anticipated with an optimization of the size distribution of the powder particles.

## Acknowledgment

We wish to acknowledge the help of Mr Marc Durand in the establishment of the X-ray diffraction study of the amalgamation reactions of Ms Marina Condemine and Sylvie Tardieu (both students at Ecole des Mines de Paris) in some of the experimental work presented here and of Gérard Frot and Maria Simoes for their careful EPMA and SEM analysis.

## References

1. K. F. LEINFELDER, *Current Opinion in Dentistry* **1** (1991) 214.
2. M. J. VIMY, A. J. LUFT and F. L. LORSCHIEDER, *J. Dent. Res.* **65**(12) (1986) 1415.
3. S. HALBACH, *ibid.* **74**(4) (1995) 1103.
4. E. BERDOUSES, T. K. VAIDYANATHAN, A. DASTANE, C. WEISEL, M. HOUP and Z. SHEY, *ibid.* **74**(5) (1995) 1185.
5. L. GERKIN, *Powder Metall. Int.* **25**(2) (1993) 59.
6. Ternary Alloys, vol. 2, (edited by G. Petzow and G. Effenberg) (VCH Publisher New York) 1988.
7. Dental Materials—Alloys for Dental Amalgam, International Standard ISO 1559 (1995).
8. W. D. KRAFT, G. PETZOW and F. ALDINGER, *Z. Metallkde.* **71** (1980) 699.
9. T. OKABE, R. J. MITCHELL, M. B. BUTTS and C. W. FAIRHURST, *J. Dent. Res.* **57** (1978) 975.
10. T. OKABE, M. B. BUTTS, J. J. HERRERNAN, E. E. KEPLER, R. J. MITCHELL and K. ASGAR, *ibid.* **59B** (1980) 969 (329).
11. E. S. DUKE, M. A. COCHRAN, B. K. MOORE and H. E. CLARK, *JADA* **105** (1982) 636.
12. R. M. GERMAN, *Powder Metallurgy Science*, 2nd edition, (MPIF, Princeton, New Jersey, USA).
13. R. TONDON and R. M. GERMAN, *Int. J. of Powder Metallurgy* **30**(4) (1994) 435.
14. K. SAIDA, Y. ZHOW and T. NORTH, *J. Materials Science* **28** (1993) 6427.
15. N. D. MC DONALD and T. W. EAGAR, *Ann. Rev. Mater. Sci.* **22** (1992) 23.
16. P. BAYARD, Ph. D. Thesis, Ecole des Mines de Paris (1997).

*Received 17 November 1998*

*and accepted 21 June 1999*